ACS APPLIED MATERIALS & INTERFACES

Letter

www.acsami.org

Channel-Length-Dependent Transport and Photovoltaic Characteristics of Carbon-Nanotube-Based, Barrier-Free Bipolar Diode

Leijing Yang,[†,‡,§] Sheng Wang,*[,†,‡] Qingsheng Zeng,[†,‡] Zhiyong Zhang,[†,‡] Yan Li,[†,⊥] Weiwei Zhou,[#] Jie Liu,[#] and Lian-Mao Peng[†,‡,*]

[†]Key Laboratory for the Physics and Chemistry of Nanodevices, [‡]Department of Electronics, [§]Academy for Advanced Interdisciplinary Studies, and [⊥]College of Chemistry and Molecular Engineering, Peking University, Beijing 100871, China

[#]Department of Chemistry, Duke University, Durham, North Carolina 27708, United States

Supporting Information

ABSTRACT: Carbon nanotube (CNT) diodes with different channel length between L = 0.6μm to 3.5 μm are fabricated on the same tube, and the electric and photovoltaic characteristics are investigated. It is found that although the open voltage of the diode increases rapidly for channel length L less than 1.0 μm, it saturates for longer channel devices. On the other hand, the short circuit current of the diode exhibites a clear peak at intermediate channel length of about 1.5 μm, a large leakage current via tunneling for short channel device and significantly decreased current for long channel device due to the increased recombination and channel resistance. The optimal channel length for a CNT diode in photovoltaic application is thus determined to be about 1.5 μm.

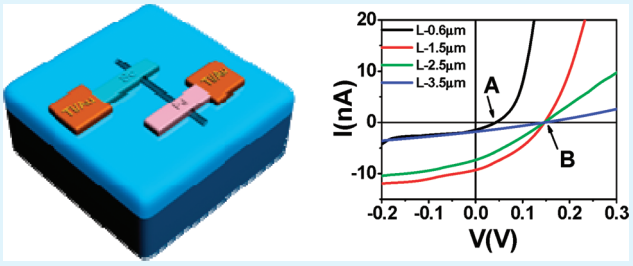

KEYWORDS: *carbon nanotube, diode, photovoltaic, channel length, doping-free*

INTRODUCTION

Optoelectronic properties of carbon nanotubes (CNTs) have attracted much attention in recent years.[1] In particular, CNTs have been investigated for various electronic and optoelectronic device applications, such as light-emitting diodes,[2,3] photodetectors, and photovoltaic (PV) cells.[4,5] Semiconducting single-wall CNTs (SWCNTs) are direct-gap materials that can efficiently absorb and emit light.[1] The unique band structure of SWCNT indicates that multiple subbands absorptions can contribute to optoelectric properties.[1] By combining sufficient nanotubes with different diameters, it was also demonstrated that it is possible to gain a nearly continuous absorption response within a broad spectral range (from UV to infrared) to match the solar spectrum.[6] In addition, extremely efficient carrier multiplication (CM) effect has been observed,[7] which may potentially lead to a higher energy conversion efficiency than that defined by the Shockley−Quiesser limit.[8] More recently, efficient photovoltage multiplication was also realized via introducing virtual contacts in CNTs, making the output photovoltage of CNT-based solar cells a tunable quantity via choosing the diameter of the tube and the number of virtual contacts introduced in the device.[9]

CNT-based PV devices have been constructed based on several device structures,[1] including p-n or p-i-n diodes[1,2,4,7,10−13] and heterojunction CNT-silicon diodes.[14−16] But most of these devices are based on chemical doping on CNTs, which may suffer from long time stability problem, or electrostatic doping using multiple splitting gates which demands complex fabrication processes and multiple power supplies. Although Schottky barrier (SB) between metal electrode and CNT, such as that in a FET device, can provide the required built-in field for separating photoexcited carriers, the SB will reduce the maximum achievable photovoltage.[1] In an earlier paper,[17] we have shown that barrier-free bipolar diode (BFBD) (see Figure 1b,c), which is made of an intrinsic SWCNT being asymmetrically contacted with Pd[18] and Sc[19] or Y,[20] behaves like a diode in dark (see Figure 1e) and may potentially be used in PV applications.[9]

Charge separation in a BFBD device is achieved by the built-in electric field established between the two asymmetric contacts as shown in Figure 1d. Under illumination, electron-hole pairs are created in the CNT channel and separated by the built-in field, leading to observed photocurrent. The total photocurrent is determined by the number of photons being absorbed by the CNT channel and the efficiency of the photoexcited electron-hole pairs are collected by electrodes. While photon absorption is dependent on the channel length, the collection efficiency is more sensitive to the built-in field or band-bending occurring in the CNT channel. In addition, the energy conversion efficiency also depends on the total series

Received: December 14, 2011
Accepted: February 10, 2012
Published: February 10, 2012

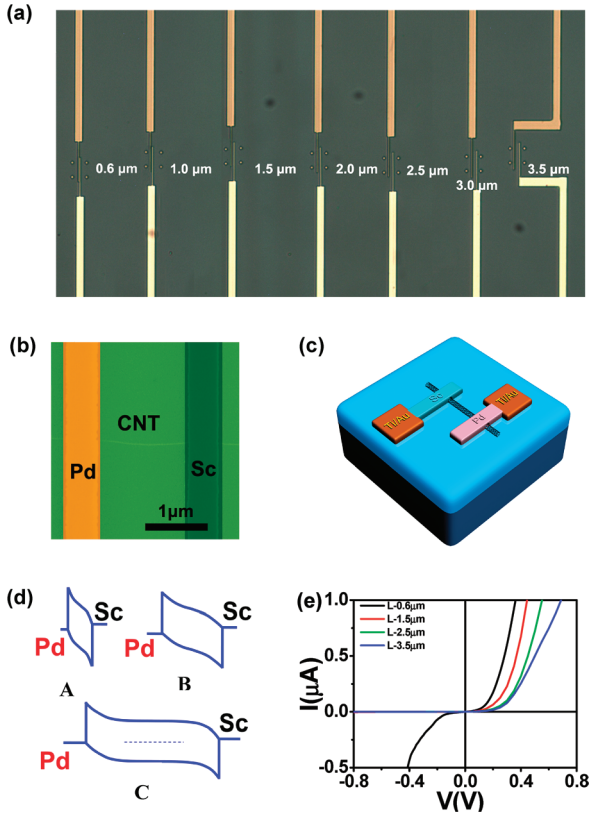

Figure 1. (a–c) Optical microscope image of seven devices with different channel length; SEM image and depicted structure of CNT-based BFBD diode. (d) Energy band diagram depicting the build-in electric field in short (panel A), immediate (panel B), and long (panel C) channel BFBDs. (e) Current voltage characteristics of four CNT diodes with a diameter of 3.1 nm and channel length $L \approx 0.6$ μm (dark), 1.5 μm (red), 2.5 μm (green), and 3.5 μm (blue).

resistance which changes with the channel length. In this letter, we report the channel length dependent transport and PV characteristics of BFBD devices, aiming to find the optimal CNT diode geometry for PV applications. We found that, under illumination, the short circuit photocurrent I_{sc} and open circuit voltage V_{oc} of BFBDs show distinct dependences on the channel length and a typical BFBD device may deliver the largest energy conversion efficiency with a channel length between 1 μm to 1.5 μm.

EXPERIMENTAL SECTION

Ultralong SWCNTs used in this work were grown on heavily n-doped Si wafers which were covered with 500 nm thick SiO_2 by chemical vapour deposition (CVD).[21] Diodes devices were fabricated with 60 nm asymmetric Sc and Pd electrodes being contacted on the CNT (Figure 1a, b) with e-beam lithography followed by a high vacuum e-beam deposition, and a standard lift-off process. All devices were fully covered with 180 nm Polymethyl Methacrylate (PMMA) to improve its long time stability. Semiconducting SWCNTs were identified via electrical field-effect measurements. The diameters of the SWCNTs were measured by atomic force microscopy (AFM) DI3100 (Veeco comapany). All electrical transport measurements were carried out with Keithley 4200 semiconductor analyzer at room temperature. Optical measurements were carried out with a probe station attached on the Raman system (Jobin Yvon/Horiba company), and the laser with $\lambda = 785$ nm was focus on the devices using a microscope objective (50×) lens. The largest power of the focused laser beam on the device is about 9.5 kW/cm^2 with spot size ~20 μm.

RESULTS AND DISCUSSION

To explore the impact of channel length on the transport properties of BFBD device, seven diodes with different channel length (L) were fabricated on the same SWCNT with a diameter of 3.1 nm. Figure 1e shows current-voltage (I–V) characteristics of four devices (out of seven devices being fabricated on the same CNT) in dark with channel lengths L = 0.6, 1.5, 2.5, and 3.5 μm. When L is increased from 0.6 μm to 3.5 μm, I–V curves shift toward higher turn-on voltages. The extracted turn-on voltages are found to increase from 0.22 to 0.34 V. Because the CNT channel diameter in these diodes is ~3.1 nm, the estimated band gap energy is ~0.22 eV.[7] The turn-on voltage increases with channel length and becomes larger than the bandgap voltage when $L > 1$ μm. This increase in turn-on voltage with channel length can be explained by the energy band diagrams shown in Figure 1d. Panels A, B, and C represent band bending for devices with short (~0.6 μm), intermediate (~1.5 μm), and long (~3.5 μm) channels, respectively. For a CNT diode with a short to intermediate channel, the electric field extends all over the channel (panels A and B in Figure 1d). But for long channel length, such as $L \approx$ 3.5 μm, the built-in field vanishes in the middle of the channel, resulting in an intrinsic CNT region in the middle of the diode. Early photocurrent image experiments also demonstrated that these built-in electric fields associated with the presence of band bending at the contacts can grow to a few hundred nanometers,[22] suggesting that the total band-bending region in our BFBD device may extend over 1μm. At very small forward bias (Figure 1d, panel A), the current is dominated by thermionic electrons and holes current from Sc and Pd electrodes. The potential barrier for both types of carriers is determined by the band gap of the CNT. But for longer channel length diodes, such as the one with $L \approx 3.5$ μm, the diode changed into p-i-n type (Figure 1d, panel C). Larger turn-on voltage is therefore needed for achieving the same current value due to the extra voltage drop over the intrinsic CNT channel as shown in Figure 1e.

We note that most devices shown in Figure 1e do not show significant leakage current at reverse bias except the device with a very short channel of $L \approx 0.6$ μm. In a BFBD device, carriers can be injected into the channel at large reverse bias because the barrier may be significantly thinned for short channel device to allow efficient tunneling leading to large leakage current (Figure 1d, panel A). But it is difficult for carriers to tunnel through the barrier in long channel devices at relative low reverse bias, e.g., for $L > 0.6$ μm and $V = -0.4$ V (Figure 1d, panels B and C).

For a high quality diode, we may neglect the shunt resistance to model the I–V characteristic of the diode in dark using the diode equation[23]

$$I_{dark} = I_s\{\exp[q(V - I_{dark}R_s)/nkT] - 1\} \quad (1)$$

where V is the bias, I_s is the reverse saturation current, R_s is the effective series resistance, q is electron charge, k is the Boltzmann constant, T is temperature, and n denotes the ideality factor of the diode. In our diodes, n is 1.16 for short channel device with $L \approx 1.5$ μm, and ~1.71 for $L \approx 3.5$ μm. This suggests that defects may increase in longer channel device, making the CNT based diode less perfect.

Figure 2a shows the light response of the same four devices as in Figure 1e. Under illumination, the four devices yield open

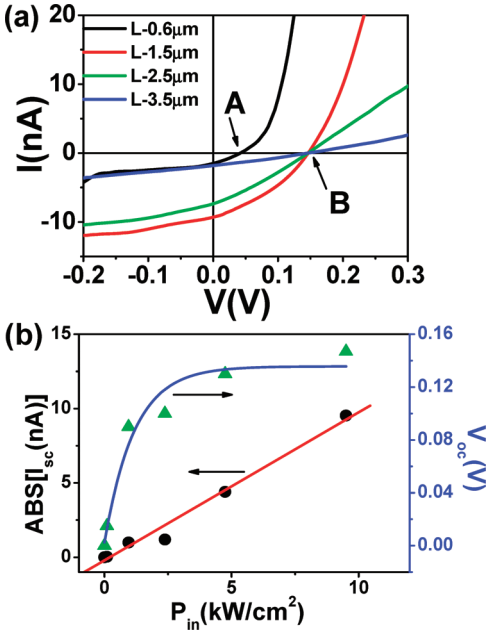

Figure 2. (a) Current−voltage characteristics of the four diodes as in Figure 1, under illumination of 9.5 kW/cm^2. (b) V_{oc} (blue) and I_{sc} (red) as functions of incident light power density for L = 1.5μm.

circuit voltage V_{oc} and short-circuit current I_{sc} values of 0.05 V and 1.6 nA (for L = 0.6 μm), 0.15 V and 9.5 nA (for L = 1.5 μm), 0.15 V and 7.4 nA (for L = 2.5 μm), and 0.15 V and 1.8 nA (for L = 3.5 μm), respectively. These data show that both V_{oc} and I_{sc} change significantly with channel length, but V_{oc} and I_{sc} do not have the same dependence on L. In Figure 2a, I_{sc} first increases with channel length for L < 1.5 μm, but starts to decrease when L > 1.5 μm. On the other hand V_{oc} increases from 0.05 V (for $L \approx$ 0.6 μm) to 0.15 V (for L = 1.5 μm) (Figure 2a, points A and B), and then remains almost unchanged from $L \approx$ 1.5−3.5 μm (see Figure 3a).

Under low illumination condition, the total current in the channel is determined by the balance between the diffusion or dark current I_{dark} and the light generated current I_{sc}. To a rough approximation the total current is given by

$$I(V) = I_{dark} - I_{sc} = I_s\{\exp[q(V - I_{dark}R_s)/nkT] - 1\} - I_{sc} \quad (2)$$

which is an illumination dependent shift of the dark current. In general, the efficiency of PV energy conversion is dependent on light absorption, charge separation, and transport (or collection) through the CNT channel. For low incident light intensity, however, the open circuit voltage depends also sensitively on the incident flux. Although the light generated current I_{sc} is not very sensitive to the bias of the CNT diode, it increases rapidly with increasing incident flux. If the incident flux b_0 is increased by a factor P_{in}, light absorption or electron-hole pair generated and thus I_{sc} will increase by the same factor, i.e., $I_{sc}(P_{in}b_0) = P_{in}I_{sc}(b_0)$, and this linear relationship is amply demonstrated in Figure 2b (red curve). When the circuit is open, the total current is zero

$$I(V_{oc}) = 0 \approx I_s[\exp(qV_{oc}/nkT) - 1] - I_{sc} \quad (3)$$

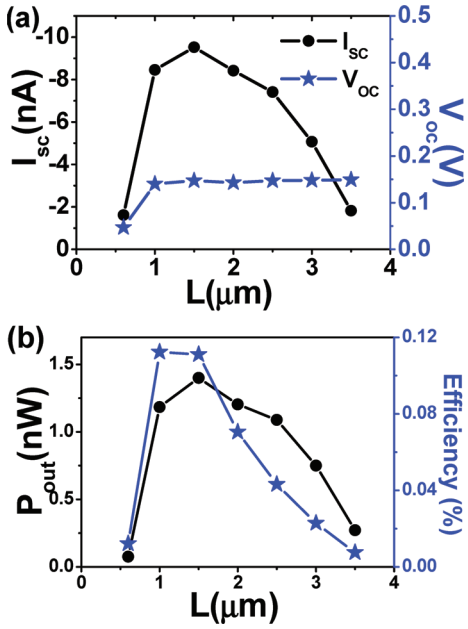

Figure 3. Channel-length-dependent (a) V_{oc} (blue) and I_{sc} (dark), (b) output power and power conversion efficiency for seven diodes with different channel lengths.

leading to the following equation for the open circuit voltage

$$V_{oc}(P_{in}) = (nkT/q)\ln[P_{in}I_{sc}(b_0)/I_s + 1] \quad (4)$$

At very low incident power, $V_{oc}(P_{in})$ increases rapidly with increasing P_{in}, but it saturates at a value about 0.15 V (Figure 2b, blue curve). It should be noted that in deriving eq 3, we have neglected the effect of the series resistance on V_{oc}, i.e., the $I_{dark}R_s$ term in eq 1. For a typical dark current of few nA and $R_s \approx 1 \times 10^5$ Ω (Figure 1e), this approximation results in a uncertainty in the bias on the order of mV, which is indeed negligible compared with the typical V_{oc} on the order of 0.1−0.2 V for CNT diodes.

For a fixed incident flux and to a good approximation, the absorbed number of photons increases also linearly with the length of the CNT channel. Assuming the CNT length is increased by a factor L, photon absorption of the CNT and thus I_{sc} as well will increase by the same factors, i.e., $I_{sc}(L) = LI_{sc}(L_0)$, yielding a photogenerated open circuit voltage

$$V_{oc}(L) = (nkT/q)\ln[LI_{sc}(L_0)/I_s + 1] \quad (5)$$

At low absorption and open circuit, the photovoltage V_{oc} builds up quickly, which in turn promotes an exponentially increasing dark current. This dark current eventually balances with the light generated current yielding a logarithmically increasing photovoltage with the length of the CNT which saturates for long CNT channel devices. Figure 2a shows that whereas for a short CNT with L = 0.6 μm, the open circuit voltage is only about 0.05 V, it saturates quickly toward 0.15 V for L equal or larger than 1.0 μm. Furthermore, reverse saturation current I_s also decreases with increasing channel length due to lower leakage current for devices with L > 1 μm. So the eq 5 also indicates that the device with L = 0.6 μm appear the least V_{oc} in these seven devices. There are two aspects attributing to the lower V_{oc} for short channel diode. The first one is relative small light absorb area corresponding limited photocarriers number. The second is that larger leakage current in diode as shown in Figure 1e. When the channel of devices is larger than 1 μm,

dx.doi.org/10.1021/am201778x | ACS Appl. Mater. Interfaces 2012, 4, 1154−1157

leakage current is declining dramatically, the V_{oc} of devices show saturation (see point B in Figure 2a). The largest V_{oc} is 0.15 V for diodes in Figure 2a, which is less than the ideal photovoltage corresponding to the band gap energy E_g of CNT, $E_g/e \approx 0.22$ V. This difference between ideal V_{oc} and the measurement might attribute to interface dipole layer on the CNT/metal interface or recombination including Auger, trap-assisted recombination and surface recombination from CNT and silicon oxide. For a very long CNT with $L \gg 1.5$ μm, while V_{oc} remains basically the same at the 0.15 V level, the short circuit current level decreases from about 9.3 nA for L=1.5 μm down to about 1.8 nA for L= 3.5 μm. This is because for a long CNT, the diode becomes a p-i-n type, and in the middle of the CNT the built-in field vanishes and recombination increases, reducing significantly the short circuit current. The channel length dependent I_{sc} and V_{oc} are shown in Figure 3a for seven devices fabricated on the same SWCNT. While the open circuit voltage saturates for L slightly larger than 1.0μm, the short circuit current reaches a maximum at L = 1.5 μm and then decreases for longer channel length devices. Therefore, the device with $L \approx 1.5$ μm has a maximum fill factor (FF) of about 0.35. Other FF of the devices are 0.10 and 0.28 for $L \approx 3.5$ μm and 0.6 μm, respectively, which may in principle be increased by reducing the series resistance R_s of the device via connecting more semiconducting CNTs in parallel as the conducting channel. In order to estimate the conversion efficiency of BFBD devices, we calculate the output power of these devices (Figure 3b) and found that the device with $L \approx 1.5$ μm has the highest power conversion efficiency η = 0.11%.

CONCLUSIONS

In summary, we have investigated the channel-length-dependent electric and photovoltaic characteristics of semiconducting CNT based diode devices. The short circuit current I_{sc} and open circuit voltage V_{oc} of the device are both found to increase rapidly for short channel devices with L < 1.0 μm, but I_{sc} and V_{oc} begin to fall or saturate at $L \approx 1.5$ μm. Hence, the optimal channel length for a CNT diode in PV application is determined to be about 1.5 μm.

ASSOCIATED CONTENT

Supporting Information

The characteristic of carbon nanotube with AFM and the details of electric and photoelectric results of diode devices are provided. This material is available free of charge via the Internet at http://pubs.acs.org/.

AUTHOR INFORMATION

Corresponding Author

*E-mail: shengwang@pku.edu.cn (S.W.); lmpeng@pku.edu.cn (L.-M.P.).

Notes

The authors declare no competing financial interest.

ACKNOWLEDGMENTS

This work was supported by the Ministry of Science and Technology (Grants 2011CB933002 and 2011CB933001), and National Science Foundation of China (Grants 61001016). Work at Duke is supported by ONR(N00014-09-1-0163).

REFERENCES

(1) Avouris, P.; Freitag, M.; Perebeinos, V. *Nat. Photonics* **2008**, *83*, 341−350.
(2) Mueller, T.; Kinoshita, M.; Steiner, M.; Perebeinos, V.; Bol, A. A.; Farmer, D. B.; Avouris, P. *Nat. Nanotechnol.* **2010**, *5*, 27−31.
(3) Wang, S.; Zeng, Q. S.; Yang, L. J.; Zhang, Z. Y.; Wang, Z. X.; Pei, T.; Ding, L.; Liang, X. L.; Gao, M.; Li, Y.; Peng, L.-M. *Nano Lett.* **2011**, *11*, 23−29.
(4) Lee, J. U. *Appl. Phys. Lett.* **2005**, *87*, 073101-1−3.
(5) Chen, C. X.; Lu, Y.; Kong, E. S.; Zhang, Y. F.; Lee, S. T. *Small* **2008**, *4*, 1313−1318.
(6) Lehman, J.; Sanders, A.; Hanssen, L.; Wilthan, B.; Zeng, J.; Jensen, C. *Nano Lett.* **2010**, *10*, 3261−3266.
(7) Gabor, N. M.; Zhong, Z. H.; Bosnick, K.; Park, J.; McEuen, P. L. *Science* **2009**, *325*, 1367−1371.
(8) Shockley, W.; Queisser, H. J. *J. Appl. Phys.* **1961**, *32*, 510−519.
(9) Yang, L.J.; Wang, S.; Zeng, Q. S.; Zhang, Z. Y.; Pei, T.; Li, Y.; Peng, L.-M. *Nat. Photonics* **2011**, *5*, 672−676.
(10) Bosnick, K.; Gabor, N.; McEuen, P. *Appl. Phys. Lett.* **2006**, *89*, 163121-1−3.
(11) Liu, C. H.; Wu, C. C.; Zhong, Z. H. *Nano Lett.* **2011**, *11*, 1782−1785.
(12) Abdula, D.; Shim, M. *ACS Nano* **2008**, *2*, 2154.
(13) Avouris, P.; Afzali, A.; Appenzeller, J.; Chen, J.; Freitag, M.; Klinke, C.; Lin, Y. -M; Tsang, J. C. *IEDM Tech. Digest* **2004**, *04*, 525.
(14) Li, Z.; Kunets, V. P.; Saini, V.; Xu, Y.; Dervishi, E.; Salamo, G. J.; Biris, A. R.; Biris, A. S. *ACS Nano* **2009**, *3*, 1407−1414.
(15) Wei, J. Q.; Jia, Y.; Shu, Q. K.; Gu, Z. Y.; Wang, K. L.; Zhuang, D. M.; Zhang, G.; Wang, Z. C.; Luo, J. B.; Cao, A. Y.; Wu, D. H. *Nano Lett.* **2007**, *7*, 2317−2321.
(16) Jia, Y.; Wei, J. Q.; Wang, K. L.; Cao, A. Y.; Shu, Q. K.; Gui, X. C.; Zhu, Y. Q.; Zhuang, D. M.; Zhang, G.; Ma, B. B.; Wang, L. D.; Liu, W. J.; Wang, Z. C.; Luo, J. B.; Wu, D. H. *Adv. Mater.* **2008**, *20*, 4594−4598.
(17) Wang, S.; Zhang, Z. Y.; Ding, L.; Liang, X. L.; Shen, J.; Xu, H. L.; Chen, Q.; Cui, R. L.; Li, Y.; Peng, L.-M. *Adv. Mater.* **2008**, *20*, 3258−3262.
(18) Javey, A.; Guo, J.; Wang, Q.; Lundstrom, M.; Dai, H. J. *Nature* **2003**, *424*, 654−657.
(19) Zhang, Z. Y.; Liang, X. L.; Wang, S.; Yao, K.; Hu, Y. F.; Zhu, Y. Z.; Chen, Q.; Zhou, W. W.; Li, Y.; Yao, Y.G.; Zhang, J.; Peng, L.-M. *Nano Lett.* **2007**, *7*, 3603−3607.
(20) Ding, L.; Wang, S.; Zhang, Z. Y.; Zeng, Q. S.; Wang, Z. X.; Pei, T.; Yang, L. J.; Liang, X. L.; Shen, J.; Chen, Q.; Cui, R. L.; Li, Y.; Peng, L.-M. *Nano Lett.* **2009**, *9*, 4209−4214.
(21) Zhou, W. W.; Han, Z.Y.; Wang, J.Y.; Zhang, Y.; Jin, Z.; Sun, X.; Zhang, Y.W.; Yan, C.H.; Li, Y. *Nano Lett.* **2006**, *6*, 2987−2990.
(22) Freitag, M.; Tsang, J. C.; Bol, A.; Yuan, D.; Liu, J.; Avouris, P. *Nano Lett.* **2007**, *7*, 2037−2042.
(23) Nelson, J. *Physics of Solar Cells*; Imperial College: London, 2003.